IOP Conf. Series: Materials Science and Engineering **785** (2020) 012022 doi:10.1088/1757-899X/785/1/012022

Application of fuzzy logic for power change rate constraint in core power control at Reaktor TRIGA PUSPATI

Mohd Sabri Minhat[1,2], Nurul Adilla Mohd Subha[1, a)], Fazilah Hassan[1], Anita Ahmad[1]

[1]School of Electrical Engineering, Faculty of Engineering, Universiti Teknologi Malaysia, 81310 Skudai, Malaysia.
[2]Reactor Instrumentation and Control Engineering, Reactor Technology Centre, Malaysian Nuclear Agency, 43000 Kajang, Malaysia.

[a]nuruladilla@utm.my

Abstract. The 1MWth Reaktor TRIGA PUSPATI (RTP) in Malaysia Nuclear Agency has been in operation more than 37 years. The existing core power control uses a conventional controller known as Feedback Control Algorithm (FCA). It is technically challenging to keep the core power output stable and operate within the acceptable error bands for the safety demand of the RTP. At present, the power tracking performance of the system could be considered unsatisfactory where constant gains of power change rate constraint and control rod speed constraint are used. Hence, a study of a new power change rate constraint design to achieve safe control rod speed range is conducted to improve the current performance. In this paper, a new power change rate constraint (PCRC) method using fuzzy logic is proposed to control the core power. The Takagi-Sugeno (T-S) type Fuzzy model is chosen due to its capability to work well with linear controller and making the computational control algorithm efficient. The model for core power control consists of mathematical models of the reactor core, FCA, and control rods selection algorithm. The mathematical models of the reactor core are based on point kinetics model, thermal-hydraulic models and reactivity models. The performance of power tracking and actuation signal for control rod drive input are compared between the conventional PCRC (cPCRC) and Fuzzy PCRC using MATLAB. In conclusion, the proposed Fuzzy PCRC has satisfactory performance in core power tracking for controlling the nuclear reactor with high reliability and safety.

1. Introduction

The current Reaktor TRIGA PUSPATI (RTP) operating at the Malaysian Nuclear Agency is a TRIGA Mark II nuclear reactor type. It is widely used as non-power nuclear reactor with applications include production of radioisotopes, neutron radiography, basic research on the properties of materials and for education and training.

The core power control is important for safe operation of the reactor and to keep the nuclear reactor operating within its safety limit at any time and under any circumstances. The malfunction of reactor control system or any serious error made by reactor operator may lead to abnormal behaviour by the reactor, namely reactivity accidents [1]. If this error occurs, it may lead to loss of control of the chain reaction in the reactor core, which results in inability to shut down the reactor and loss of integrity of any barriers that prevent the release of radioactive fission products. Thus, the malfunction of control system has drawn attention to the researcher in developing and designing the core power control to constraint reactor safety parameter for safe and reliable operation of the nuclear reactor.

The most common safety parameter constraints such as reactivity limiting [2], reactor period limiting [3], power change rate limiting [4] and control rod speed limiting [5][6] are used to design robust core power control. Single control rod speed constraint is the most popular safety constraint which is much easier to design for implementation in a practical system. Hence, in this paper, both control rod speed and power change rate constraints will be considered to improve the tracking performance at RTP.

The RTP uses a conventional controller known as Feedback Control Algorithm (FCA) [7] which is capable to control core power up to 1MW based on conventional power change rate constraint (cPCRC). Currently, the power control system is employing a constant gain in cPCRC. However, this method yield unsatisfactory power tracking performance due to its frequent control rod movements which due to power oscillations and longer settling time to reach power demand. To solve this problem, a Takagi-Sugeno (T-S) type fuzzy approach has been established as in [8]. The fuzzy approach is chosen due to its capability to work well with a linear controller and making the computational control algorithm more efficient [9].

The power change rate is considered in designing the core power control in nuclear reactor for safe operation and within the safety limits. A few studies on power change rate constraints in core power control have been carried out. For example, in [10] and [11], a robust nonlinear Model Predictive Control (MPC) is designed by considering the optimization constraints such as xenon oscillation and maximum control rod speed. However, this method requires excessive computational effort in the on-line application.

In addition, although there are several methods dealing with the power change rate constraint which have been developed by using a reactor power profile such as the sigmoidal type trajectory in [12] and [13], these methods are not applicable for practical application since the user need to generate the appropriate load profile which significantly increases the sensitivity to input variations on the system. To cater this issue, the fuzzy-based power change rate constraint has been proposed based on tangential and sigmoid function [4]. However, the presented results require more computational time and still can be further optimized. Furthermore, in the aforementioned works [10-13], only the control rod speed (reactivity insertion) constraint is considered for the core power control.

In this paper, the power change rate constraint using fuzzy logic based on simplest linear membership function is proposed which lead to significant improvements such as applicability as a practical system, easy setting of limiting condition value for safe operation and less computational time consumption. Also, multiple constraint parameters combination of power change rate and control rod speed have been studied.

This paper is organized as follows. The modelling of RTP is presented in section 2 and the RTP core power control system is briefly described in section 3. The conventional power change rate constraint (cPCRC) and Fuzzy PCRC designs are presented in section 4. The experiment results and discussion on the implementation of cPCRC and Fuzzy PCRC to RTP model are given in section 5. Finally, conclusions are at the end of the paper.

2. Modelling of Reaktor TRIGA PUSPATI

2.1. Non-linear model

The point reactor core for a TRIGA Mark II reactor has been already modelled by [14] and is derived based on the combination of point kinetic, thermal-hydraulic and reactivity equations. The reactor core model can be simplified as:

$$\left.\begin{aligned}
\frac{d\psi}{dt} &= \frac{\rho-\beta}{\Lambda}\psi + \sum_{i=1}^{6}\lambda_i\eta_i \\
\frac{d\eta_i}{dt} &= \frac{\beta_i}{\Lambda}\psi - \lambda_i\eta_i \quad i = 1, \dots, 6 \\
\frac{dT_m}{dt} &= \frac{N_0(1-f)}{M_m C_m} + \frac{T_f - T_m}{M_m C_m/K} - \frac{\Gamma}{M_m}(T_m - T_{in}) \\
\frac{dT_f}{dt} &= \frac{N_0 f}{M_f C_f} - \frac{T_f - T_m}{M_f C_f/K} \\
T_m &= wT_{out} + (1-w)T_{in} \\
\Gamma &= \frac{Kw(T_f - T_m)}{C_m(T_m - T_{in})} \\
\rho &= a_h \Delta h_{cr} + \alpha_m(T_m - T_m^0) + \alpha_f(T_f - T_f^0) \\
\delta\dot{\rho}_r &= W z_d
\end{aligned}\right\} \tag{1}$$

The actual core power, N, can be expressed as [15]:

$$N = \psi N_0 \tag{2}$$

All the parameters used in this paper are summarized in Table 1.

Table 1. Nomenclature for equations 1 and 2.

ψ	Relative neutron density	β	The total fraction of effective delayed neutron (*Δk/k*)
W	Reactivity worth of the control rod bank (m^{-1})	β_i	The *i*-th group of the delayed neutron (*Δk/k*)
N_0	Nominal core power (*W*)	α_f	Reactivity due to change in temperature fuel (*Δk/k/°C*)
N	Actual core power (*W*)	α_m	Reactivity due to change in temperature moderator (*Δk/k/°C*)
C_m	Moderator specific heat capacity ($J\ kg^{-1}K^{-1}$)	η_i	The *i*-th group of normalized precursor concentration (m^{-3})
C_f	Fuel specific heat capacity ($J\ kg^{-1}K^{-1}$)	T_f	Average temperature of fuel (°*C*)
M_m	Moderator total mass (*kg*)	T_f^0	Average temperature of fuel at initial equilibrium state (°*C*)
M_f	Fuel total mass (*kg*)	ρ	Total reactivity
Γ	Coolant mass flow rate (kgs^{-1})	$\delta\rho_r$	Reactivity produced by the movement of the control rod bank
K	Global heat transfer coefficient ($W\ {}^0C^{-1}$)	T_{out}	Average outlet temperature of coolant (°*C*)
λ_i	Decay constant of the *i*-th group of delay neutron precursor (s^{-1})	T_m	Average temperature of coolant (°*C*)
w	Weighting factor for computation of moderator temperature	T_m^0	Average temperature of coolant at initial equilibrium state (°*C*)
f	Fraction of power deposited in the fuel	T_{in}	Average inlet temperature of coolant (°*C*)
Λ	Mean neutron generation time (*s*)	z_d	Velocity of the control rod bank (ms^{-1})
a_h	Reactivity worth of the control rod (*Δk/k/m*)	Δh_{cr}	Control rod position differences from the critical position (*m*)

3. RTP core power control system

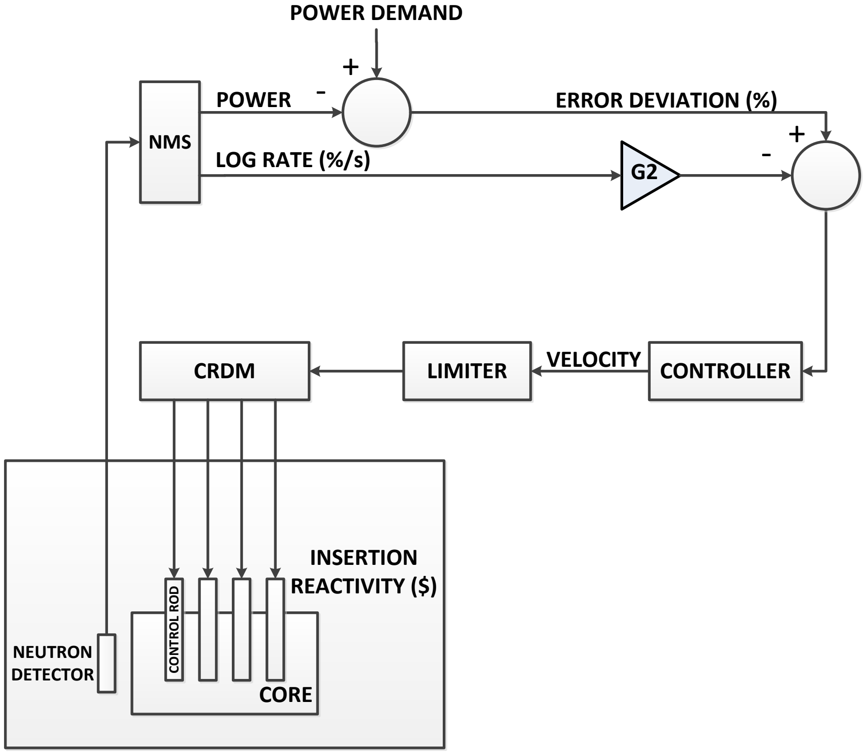

Figure 1. Block Diagram of Core Power Control System in RTP.

The closed-loop block diagram of the core power control system in RTP known as Feedback Control Algorithm (FCA) is illustrated in Figure 1. The input for this system is the Power Demand (PDM) and the output is the measured thermal neutron power from the core. The neutron detector feeds Neutron Measurement System (NMS) in which processed signals are used to provide measurements of the core power (*N*) and the rate of power change (Log Rate). The error between the PDM and the power output, and then constant gain rate (*G2*) represents the conventional power change rate constraint (cPCRC) are used as the inputs for the RTP controller. The output from the controller which is the control rod velocity is fed to the velocity limiter to constraint the reactivity insertion rate in the core. Only one control rod is allowed to move (inserted to or withdrawn from the core using Control Rod Drive Mechanism, CRDM) at any one time at the speed of 2 mm/s, equals to 0.4071 mm/cycle. To date, by using cPCRC, the core power control has 1% full power chattering error with longer settling time when the reactor power is increased in the case of a sudden change in power demand.

In order to improve the core power control performance, the new design of PCRC is proposed and the FCA parameters need to be taken into account during the design stage. The FCA parameters are given in Eq. 3 [16]

$$\left.\begin{aligned} u_{PI} &= (\mathrm{G3})E + (\mathrm{G4})\int_{t_0}^{t} Edt \\ E &= \left[(\mathrm{G1})log\left(\frac{\mathrm{PDM}}{N}\right)\right]_{\pm 1} - (\mathrm{G2})\frac{1}{N}\frac{dN}{dt} \end{aligned}\right\} \tag{3}$$

where *G1*, *G2*, *G3*, and *G4* are the control gains used as constraints to limit the power change rate at below 12.5% Full Power (FP)/s limit, *E* is the error signal in terms of step numbers, t_0 is start time to calculate error signal, and t is final time (time interval) to calculate error signal. The output of the Proportional-Integral (PI) controller which determines the control rod velocity, u_{PI}, is made by using Eq. 3. The details of the RTP core power control system is illustrated in Figure 2 [17].

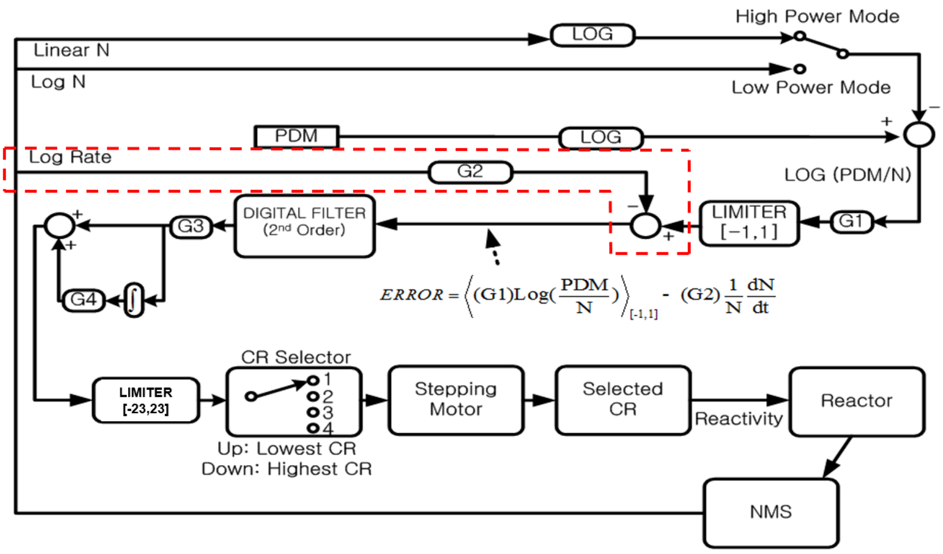

Figure 2. Details of RTP power core control system.

4. Conventional PCRC (cPCRC) and fuzzy PCRC

In this section, a new method of PCRC is proposed using fuzzy logic so that the power change rate can remain below the critical value in order to maintain the safe operation of the reactor. Due to the insertion and withdrawal motion of the control rods, the power change rate plays an important role in the core power control system. The characteristic exponential rise of the reactor power is defined in the following:

$$N(t) = N_0 e^{\frac{t}{\tau}} \tag{4}$$

where the reactor period τ is defined as the time taken for the reactor power to rise by a factor of *e* which is the base of the natural logarithm. From Eq. 4, it can be derived as:

$$ln\left(\frac{N}{N_0}\right) = \frac{t}{\tau} \tag{5}$$

Therefore, the power change rate signal over the time interval *t* can be defined as:

$$\xi_{rate} = \frac{d\, ln\, N}{dt} = \frac{1}{N}\frac{dN}{dt} = \frac{1}{\tau} \tag{6}$$

From Eq. 6, the power change rate signal should be limited to a certain level during the whole control process. Therefore, the cPCRC from Figure 2 is given in the following equation;

$$(\xi_{rate})_{constraint} = \left[G2\frac{1}{N}\frac{dN}{dt}\right]_{\pm 1} \tag{7}$$

To observe the limitation of cPCRC, the constant gain (*G2*) of Eq. 7 was set to 0.08 (12.5%/s) and then to 0.064 (15.63%/s). The visual comparison of the two different gains is illustrated in Figure 3.

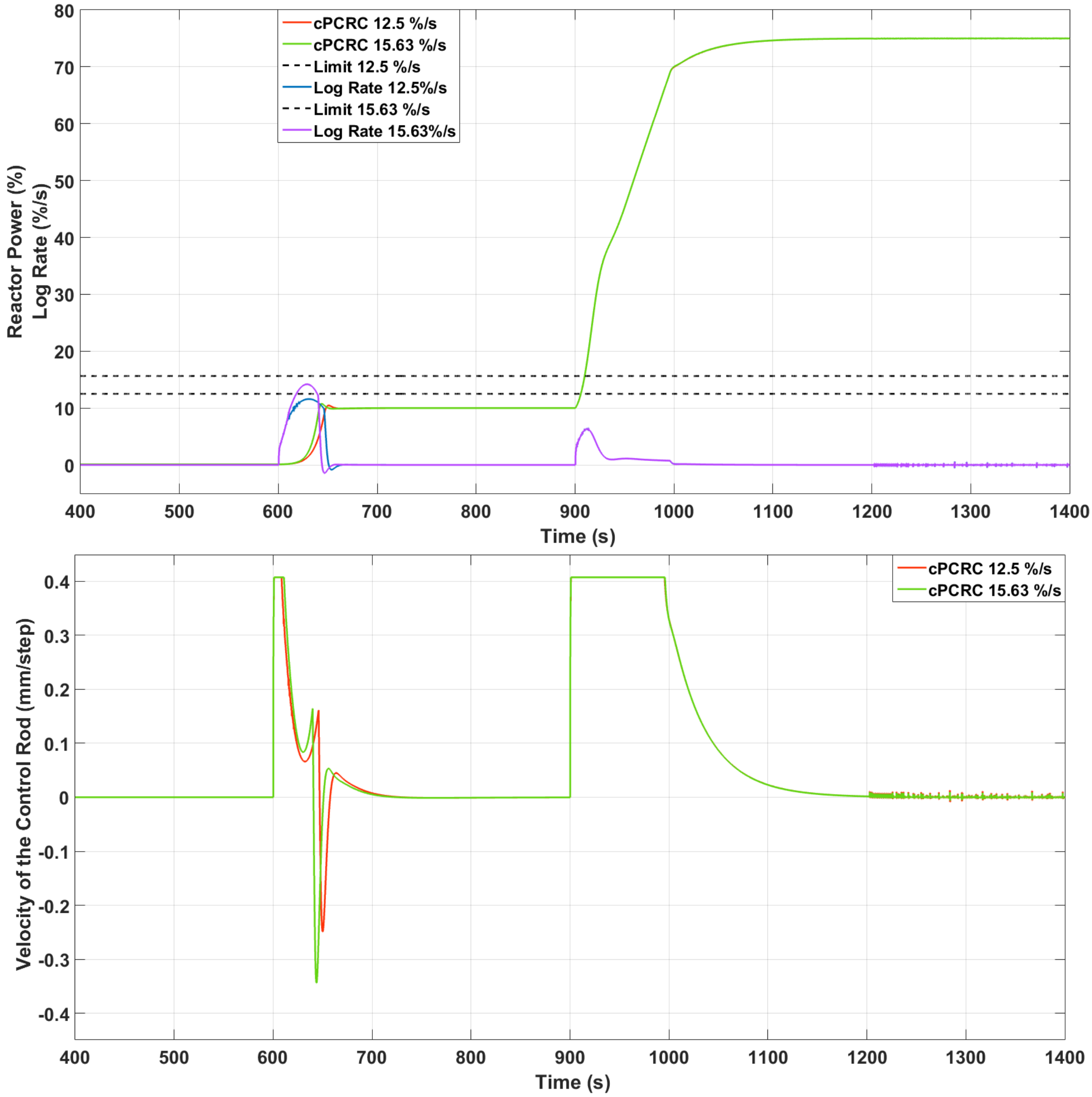

Figure 3. Comparison of different log rate values to limit the rate of power increment.

By referring to Figure 3, it is proven that increasing power change rate constraint gain in Eq. 7 has no noticeable effect on tracking control performance. However, there is a small overshoot at 10% FP.

In RTP, the cPCRC uses a single constant gain for various steps of power changes. Both the higher and lower rate of power change values give a small penalty to reduce control rod speed. In case of emergency, the maximum value of the power change rate constraint is set to 33.3% FP/s [18] using independent reactor protection system (RPS) so that the power increase can be terminated by shutting down the system to prevent the reactor power from increasing to dangerous level.

The Fuzzy PCRC uses different weighted gain constant for various step power change in which the design is using knowledge-based decision making by capitalizing operator experience. The control rod speed can be varied at different levels of penalty based on the rate of power change. The structure of

Fuzzy PCRC is illustrated in Figure 4. The output from the velocity limiter is fed to Fuzzy-Based Power Change Rate Limiter. The output from the second limiter is then applied to the control rod drive mechanism (CRDM). The advantage of this new structure is to eliminate the presence of unconsidered power change rate constraints after the controller implements the cPCRC. Furthermore, the power change rate can be adjusted to an appropriate level and thus in this work, it is set to be constrained within ±12.5% FP/s as predetermined safety limit by the Final Safety Analysis Report [18].

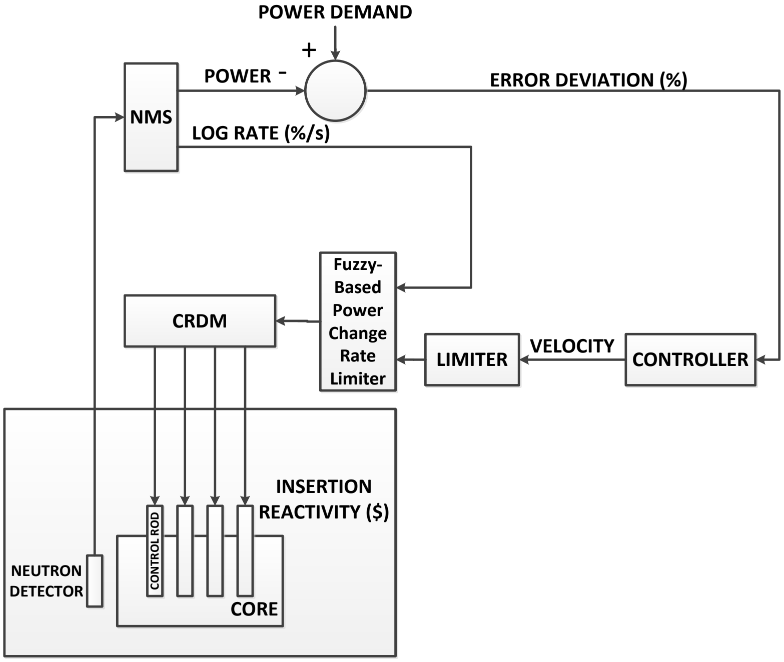

Figure 4. Block Diagram of Core Power Control using Fuzzy PCRC.

In fuzzy systems, the most commonly used parameterized membership functions are triangles (straight lines), trapezoids, bell curves, Gaussian, and sigmoidal function [19]. In this paper, three types of membership functions are studied; straight lines, bell curves and Gaussian.

The membership functions are formed using straight lines for Fuzzy PCRC as depicted in Figure 5. These straight lines of membership functions have the advantage of their simplicity.

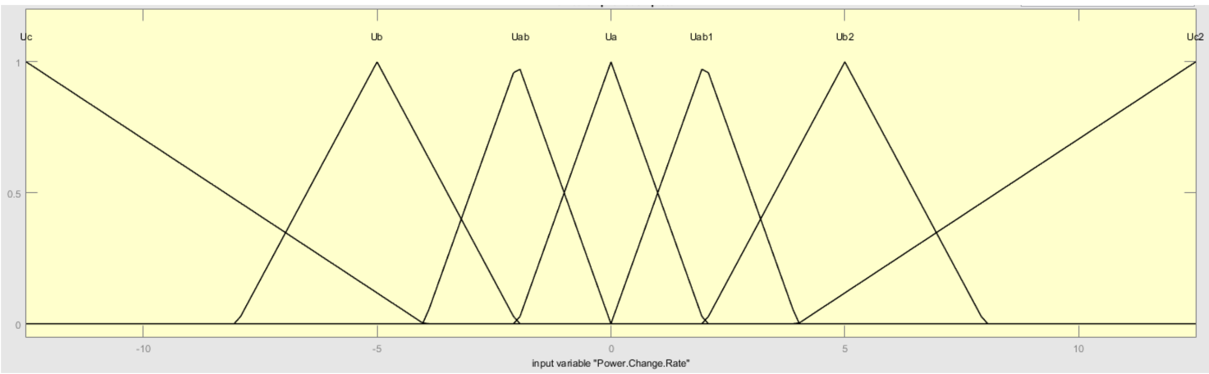

Figure 5. Straight line membership functions for Fuzzy PCRC.

The straight line membership functions for Fuzzy PCRC consists of four fuzzy sets where a power change rate ξ_{rate} is given as input variable and are introduced as follows [20].

$$\left.\begin{aligned}
u_a = f(\xi_{rate}; a_a, 0, c_a) &= \begin{cases} 0, & \xi_{rate} \le a_a \\ -\frac{\xi_{rate}-a_a}{a_a}, & a_a < \xi_{rate} < 0 \\ \xi_{rate}, & \xi_{rate} = 0 \\ \frac{c_a-\xi_{rate}}{c_a}, & 0 < \xi_{rate} < c_a \\ 0, & \xi_{rate} \ge c_a \end{cases} \\
u_{ab} = f(\xi_{rate}; a_{ab}, b_{ab}, 0) &= \begin{cases} 0, & \xi_{rate} \le a_{ab} \\ \frac{\xi_{rate}-a_{ab}}{b_{ab}-a_{ab}}, & a_{ab} < \xi_{rate} < b_{ab} \\ \xi_{rate}, & \xi_{rate} = b_{ab} \\ \frac{\xi_{rate}}{b_{ab}}, & b_{ab} < \xi_{rate} < 0 \\ 0, & \xi_{rate} \ge 0 \end{cases} \\
u_b = f(\xi_{rate}; a_b, b_b, c_b) &= \begin{cases} 0, & \xi_{rate} \le a_b \\ \frac{\xi_{rate}-a_b}{b_b-a_b}, & a_b < \xi_{rate} < b_b \\ \xi_{rate}, & \xi_{rate} = b_b \\ \frac{c_b-\xi_{rate}}{c_b-b_b}, & b_b < \xi_{rate} < c_b \\ 0, & \xi_{rate} \ge c_b \end{cases} \\
u_c = f(\xi_{rate}; a_c, b_c, c_c) &= \begin{cases} 0, & \xi_{rate} \le a_c \\ \frac{\xi_{rate}-a_c}{b_c-a_c}, & a_c < \xi_{rate} < b_c \\ \xi_{rate}, & \xi_{rate} = b_c \\ \frac{c_c-\xi_{rate}}{c_c-b_c}, & b_c < \xi_{rate} < c_c \\ 0, & \xi_{rate} \ge c_c \end{cases}
\end{aligned}\right\} \quad (8)$$

where a_i, b_i, and c_i (for $i = a, ab, b, c$) are chosen as the lower limit, the center, and the upper limit respectively of the membership functions. Before applying the implication fuzzy operator, the rule weight need to assigned first. Each rules has weight, w_i is a number from 0 through 1.0, which is applied to each part of the antecedent (a single fuzzy degree of membership between 0 and 1.0) is satisfied for each rule. Generally, this w_i is 1.0 and thus has no effect on the implication process. However, in this study changing its weight value to something other than 1.0 can decrease the effect of one rule relative to the others. The variable w_i (for $i = 1, 2, 3, 4$) is adjustable weighting parameter and can be varied at different levels of penalty based on the rate of power change. The proper w_i has been assigned to each rule based on resulting input-output surface in Figure 7 on Fuzzy PCRC (straight line). The fuzzy rules for straight lines membership functions are expressed as:

$$\left.\begin{array}{r}
Rule\ 1. If\ (Power.Change.Rate\ is\ u_c)\ then\ (output1\ is\ V_s^3)\ (w_3 = 1.0) \\
Rule\ 2. If\ (Power.Change.Rate\ is\ u_b)\ then\ (output1\ is\ V_s^2)\ (w_2 = 0.15) \\
Rule\ 3. If\ (Power.Change.Rate\ is\ u_{ab})\ then\ (output1\ is\ V_s^4)\ (w_4 = 0.01) \\
Rule\ 4. If\ (Power.Change.Rate\ is\ u_a)\ then\ (output1\ is\ V_s^1)\ (w_1 = 0.001) \\
Rule\ 5. If\ (Power.Change.Rate\ is\ u_{ab1})\ then\ (output1\ is\ V_s^4)\ (w_4 = 0.01) \\
Rule\ 6. If\ (Power.Change.Rate\ is\ u_{b2})\ then\ (output1\ is\ V_s^2)\ (w_2 = 0.15) \\
Rule\ 7. If\ (Power.Change.Rate\ is\ u_{c2})\ then\ (output1\ is\ V_s^3)\ (w_3 = 1.0)
\end{array}\right\} \quad (9)$$

The complex membership functions used for the power change rate constraint at the nuclear reactor is already modeled by [4]:

$$\left.\begin{aligned} u_a &= -0.5\, tanh\big(0.8(|\xi_{rate}| - c_1)\big) + 0.5 \\ u_b &= \frac{1}{\left|1+\left[\frac{|\xi_{rate}|-c_2}{1.2}\right]^6\right|} + 0.5 \\ u_c &= 0.5\, tanh\big(0.8(|\xi_{rate}| - c_3)\big) + 0.5 \end{aligned}\right\} \tag{10}$$

where c_1, c_2, and c_3 are chosen as the center of the membership functions. The hyperbolic tangent [21] and sigmoidal function [22] can be defined in terms of the exponential function as

$$\left.\begin{aligned} tanh(|\xi_{rate}|) &= \frac{2}{1+e^{-2|\xi_{rate}|}} - 1 \\ sigmoid(|\xi_{rate}|) &= \frac{1}{1+e^{-a(|\xi_{rate}|-c)}} \end{aligned}\right\} \tag{11}$$

In [4], the proposed method using complex functions such as hyperbolic tangent and sigmoid function for power change rate constraint is useful in adjusting the constraint bound but is computationally expensive and does not add any more precision. Thus, in reactor core power control, a simple symmetric function is preferable in building the membership function. The two membership functions are built upon the second proposed Fuzzy PCRC: a simple Gaussian curve [20] and a generalized bell curve [23].

In Figure 6, the membership functions are formed based on a simple Gaussian curve and generalized bell curve. Both Gaussian and bell membership functions are popular methods for specifying the fuzzy sets. Both curves have the advantage of being smooth and nonzero at all points.

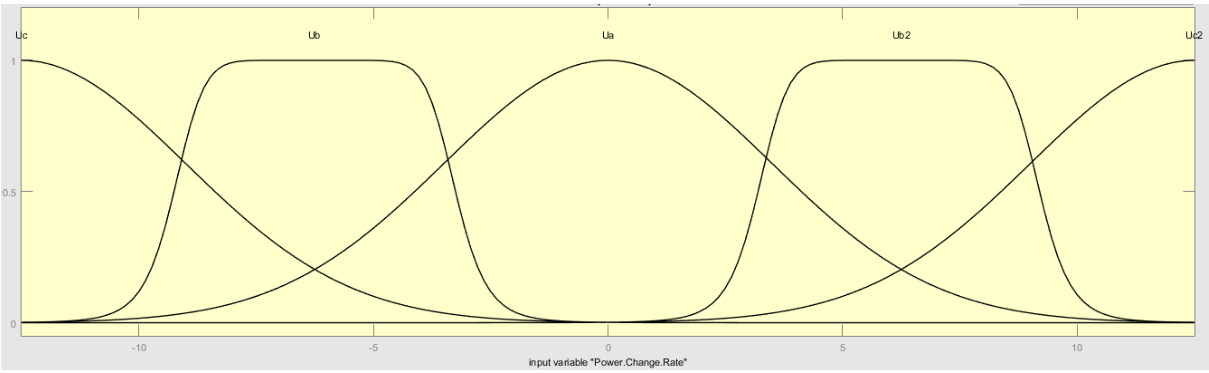

Figure 6. Gaussian and bell curves membership functions for Fuzzy PCRC.

The proposed membership functions in Figure 6 can be expressed as:

$$\left.\begin{aligned} u_a &= e^{-\frac{(|\xi_{rate}|)^2}{2\sigma^2}} \\ u_b &= \frac{1}{\left|1+\left[\frac{|\xi_{rate}|-c_b}{a}\right]^{2b}\right|} \\ u_c &= e^{-\frac{(|\xi_{rate}|-c_c)^2}{2\sigma^2}} \end{aligned}\right\} \tag{12}$$

where c_b, and c_c are positive constants and are chosen as the center of the membership functions.

In addition, the following scaled control inputs are considered:

$$V_s^i = w_i u_{step} \tag{13}$$

where w_i (for $i = 1, 2, 3$) is an adjustable weighting parameter for the constraint of the power change rate based on resulting input-output surface in Figure 7 on Fuzzy PCRC (Gaussian and bell curve). The fuzzy rule bases for Gaussian and bell curves membership functions are then expressed as

$$\left.\begin{array}{l} Rule\ 1. If\ (Power.Change.Rate\ is\ u_c)\ then\ (output1\ is\ V_s^3)\ (w_3 = 1.0) \\ Rule\ 2. If\ (Power.Change.Rate\ is\ u_b)\ then\ (output1\ is\ V_s^2)\ (w_2 = 0.5) \\ Rule\ 3. If\ (Power.Change.Rate\ is\ u_a)\ then\ (output1\ is\ V_s^1)\ (w_1 = 0.001) \\ Rule\ 4. If\ (Power.Change.Rate\ is\ u_{b2})\ then\ (output1\ is\ V_s^2)\ (w_2 = 0.5) \\ Rule\ 5. If\ (Power.Change.Rate\ is\ u_{c2})\ then\ (output1\ is\ V_s^3)\ (w_3 = 1.0) \end{array}\right\} \quad (14)$$

Then, using a center-average defuzzifier [8], a Fuzzy PCRC is designed separately for both straight lines and Gaussian and bell curves membership functions as follows:

$$\hat{u}_{step} = u_{step} - \left(\frac{u_a V_s^1 + u_b V_s^2 + u_c V_s^3 + u_{ab} V_s^4}{u_a + u_b + u_c + u_{ab}}\right) \Rightarrow \hat{u}_{step} = \left[1 - \left(\frac{u_a w_1 + u_b w_2 + u_c w_3 + u_{ab} w_4}{u_a + u_b + u_c + u_{ab}}\right)\right] u_{step} \quad (15)$$

By referring to Eq. 12, if the rate of power change is large, the membership function u_c becomes dominant i.e., have large value. In order to limit the rate, the scaled control input V_s in Eq. 13 is introduced by multiplying the weighting parameter, $w_{i=3}$ in Eq. 14 with the control rod speed is calculated by the controller, u_{step}. The larger value of V_s consequently changed and penalized the final control input $\hat{u}_{step}$ in Eq. 15 to become zero. Therefore, it can be noticed that the control of the rate of power change can be effectively accommodated in the design of the constrained control input. The Fuzzy PCRC has the advantage that adjust the constraint bound more easily compared to the cPCRC. The adjustment of the constraint bound in this work should also be investigated for three other types of PCRC control surfaces as shown in Figure 7 when considering the choice of rules and membership functions in the design stage. Then, only one input-output surface is to be selected to fit as a solution for the problem at cPCRC.

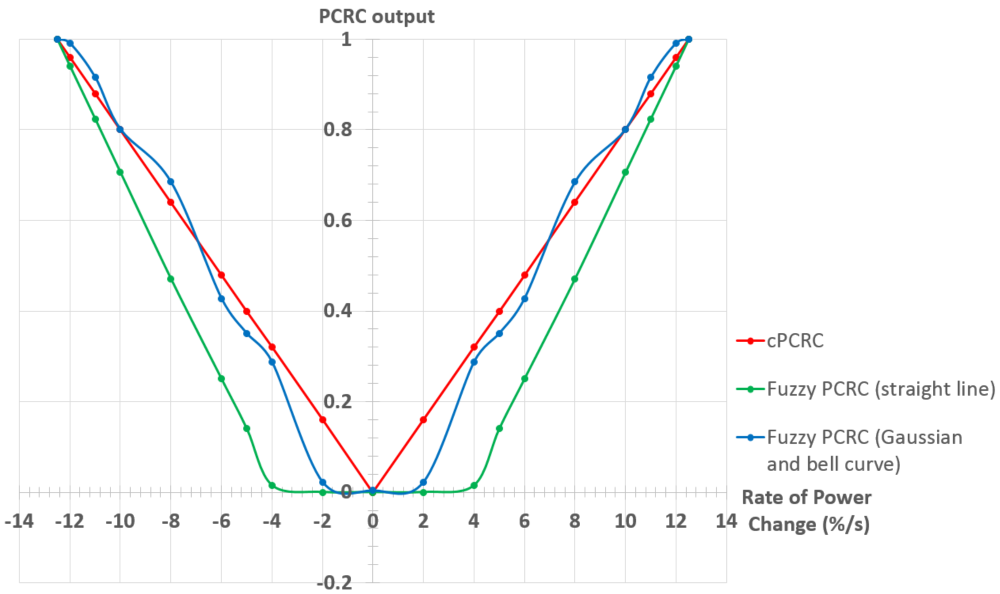

Figure 7. Comparison of different PCRC for limiting the input-output surface.

5. Experiment results and discussion

It is recommended to start a design procedure with the linear surface and then tune the gains. Figure 8 shows the overall results for the core power control performance with different PCRCs. By referring to Figures 9 to 11, the performance of all PCRC methods are observed at three different scenarios; by increasing the power to 10% FP, by reducing the power to a low power (50% FP to 10% FP) and by increasing the power to 75% FP respectively.

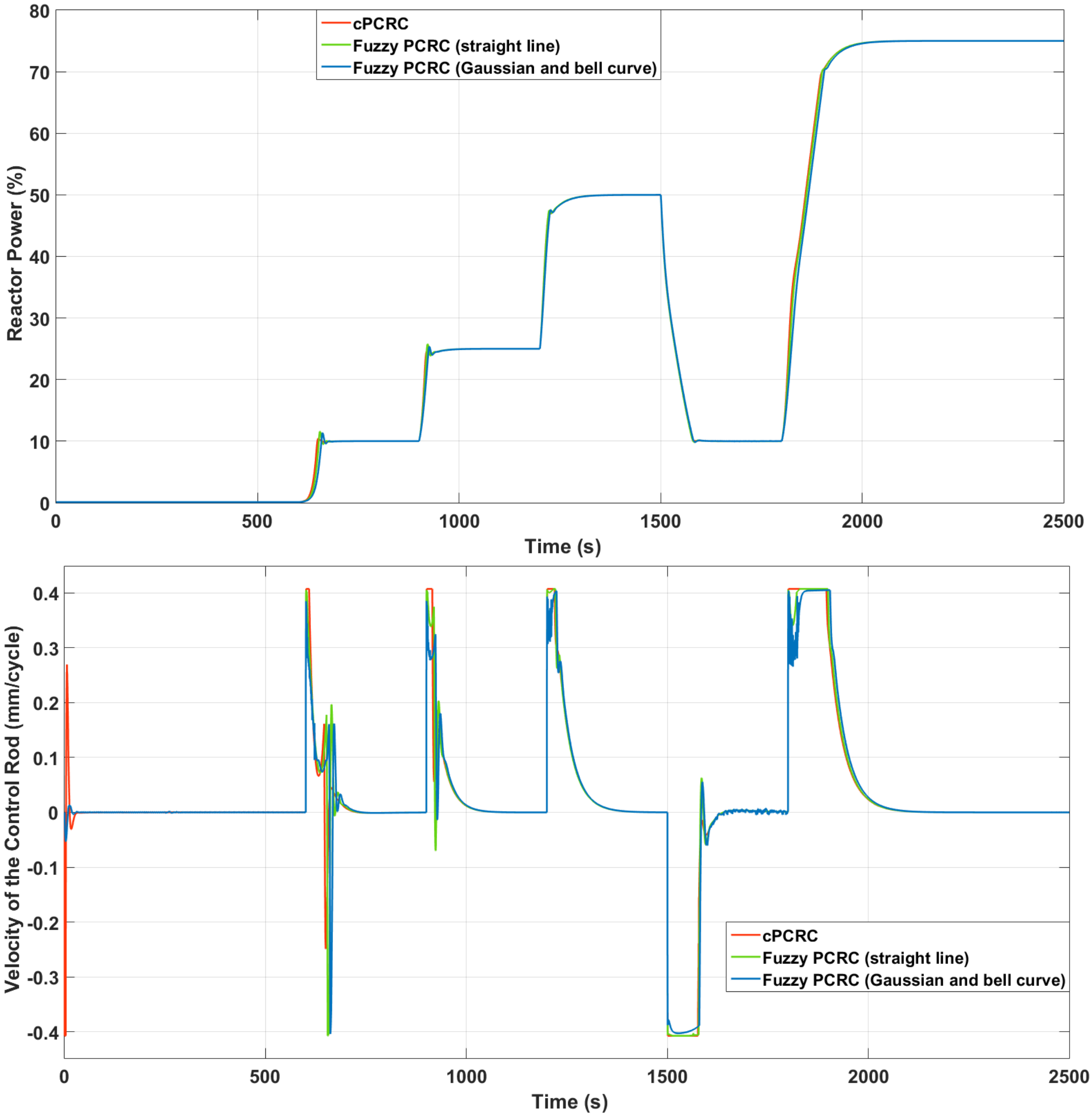

Figure 8. Comparison of different PCRC for limiting the rate of power increment at various steps of power change.

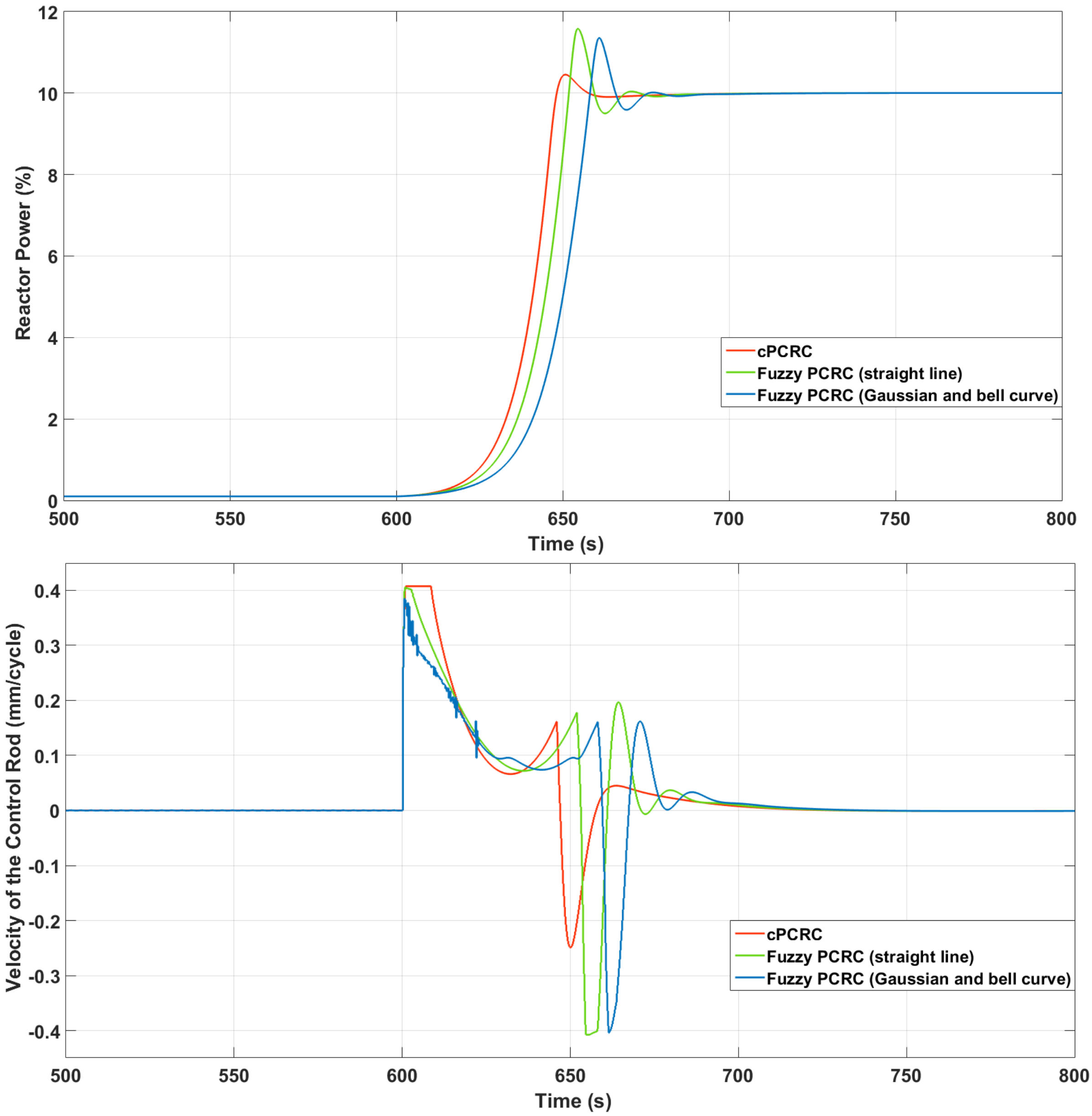

Figure 9. Comparison of different PCRC methods for limiting the rate of power increment (by increasing the power to 10% FP).

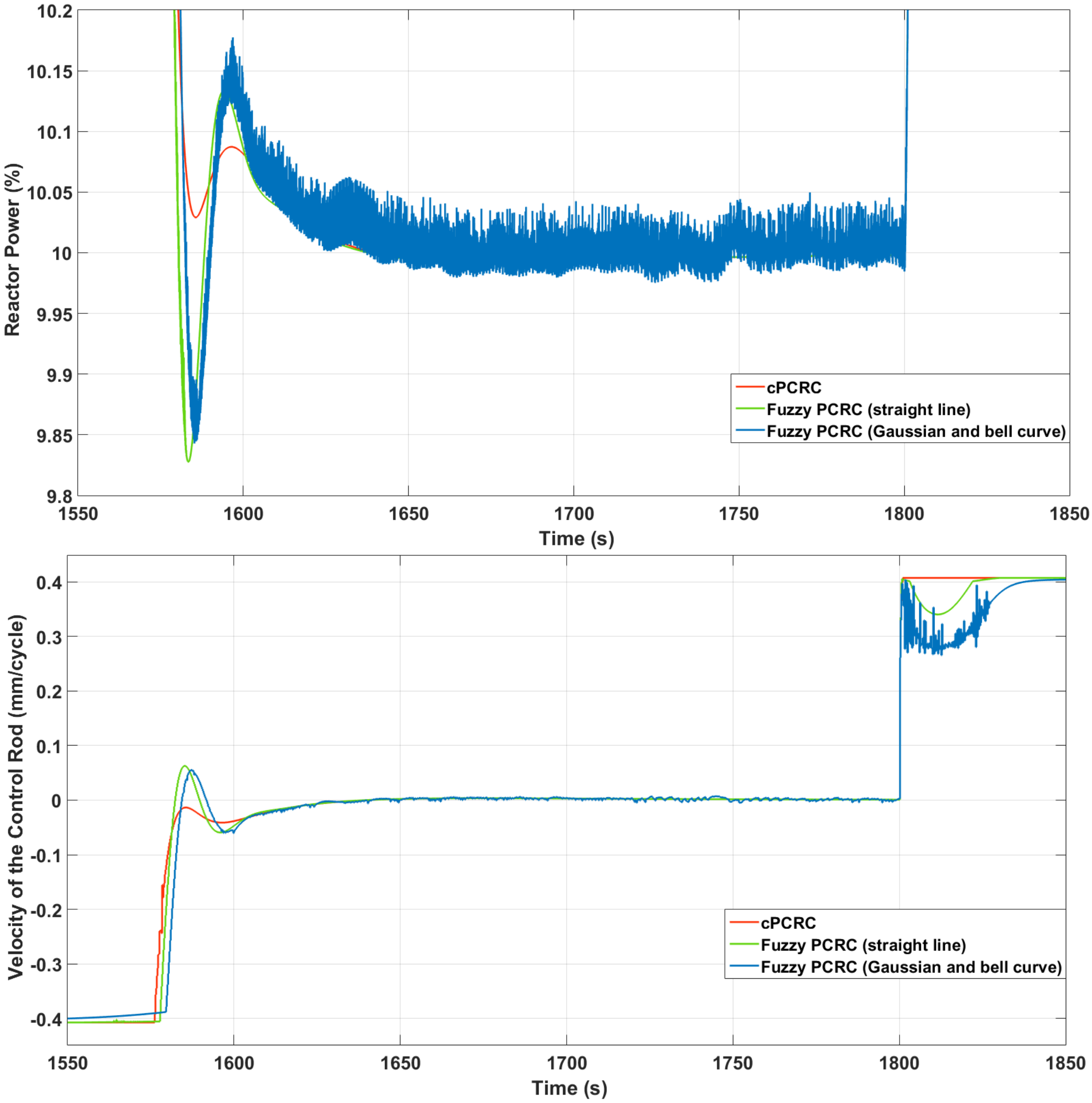

Figure 10. Comparison of different PCRC methods to limit the rate of power increment (by reducing the power to a lower power at 10% FP).

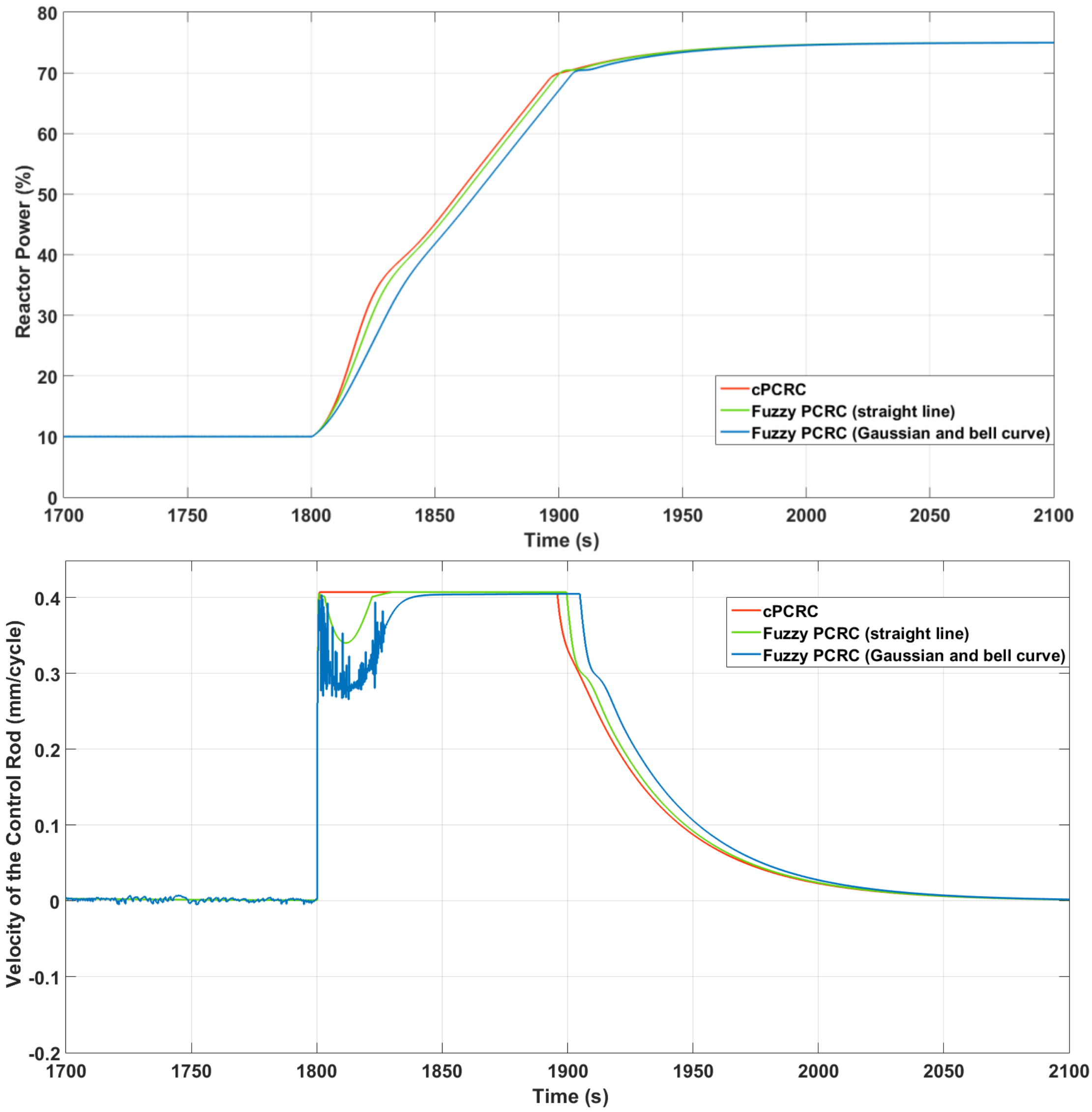

Figure 11. Comparison of different PCRC for limiting the rate of power increment (by increasing the power to 75% FP).

From Figures 8 to 11, it can be seen that the Fuzzy PCRC with straight line membership function has a gently sloping surface which will make the design more robust but with high overshoot at low power. Furthermore, this Fuzzy PCRC also is able to provide almost similar tracking to cPCRC at high and low powers within acceptable limits. On the contrary, the Fuzzy PCRC with Gaussian and bell curves membership function has tighter control with steep surface which would make the system become more oscillatory [24]. Its aggressive signal may increase the possibility of damage in CRDM. Only the Fuzzy PCRC (straight line) can significantly reduce the chattering error in the actuator during steady-state condition while others could not.

From the results above, it can be concluded that the single linear function type or the simplest triangles membership functions can produce a better control performance. In addition, the exponential function is computationally expensive, hard to be applied, non-linear in nature and is not capable of outputting a true zero (i.e., nonzero at all point). In contrast, the linear function is easier to compute and optimize. It converges faster compared to the smooth function by around a factor of six. The consideration of linear and complex membership functions in this work is to investigate the potential of both functions in improving the performance of core power control system.

Performance comparison between cPCRC and Fuzzy PCRC (straight line) at 75% FP is tabulated in Table 2 quantitatively.

Table 2. Transient and steady-state response for core power control at 750kW

Properties	*cPCRC*	*Fuzzy PCRC (straight line)*
Average (%)	74.971%	74.973%
Min (%)	74.635%	74.637%
Max (%)	75.018%	75.001%
Δe_{ce} (%)	0.383%	0.365%
Settling Time (T_s)	118.5 s	119.0 s
Percent Overshoot (%)	0.024%	0.002%
Rise Time (T_r)	84.5 s	86.0 s

From the experimental result obtained to ensure a stable power with small oscillation can be observed by measured the average, minimum and maximum value of power level during steady-state at 75% FP in a short time range; 2000 s to 2500 s. The deviation chattering error Δe_{ce} can be calculated based on the difference between maximum and minimum values. During transient, the power tracking performance can be evaluated based on the minimum value of rise time T_r and settling time T_s, where T_s is time it takes for the error between reactor power and the power demand to fall to within 5%, and T_r is time it takes for the response to rise from 10% to 90% of the steady state response. The percent overshoot is the difference between peak value and power demand as a final value in percentage.

From Table 2, it can be observed that the proposed Fuzzy PCRC (straight line) is still unable to reduce the settling time for a better power tracking performance. Due to this, a new value of control rod speed limiter was investigated for Fuzzy PCRC (straight line). The performance of cPCRC at different control rod speed constraint is shown in Figure 12.

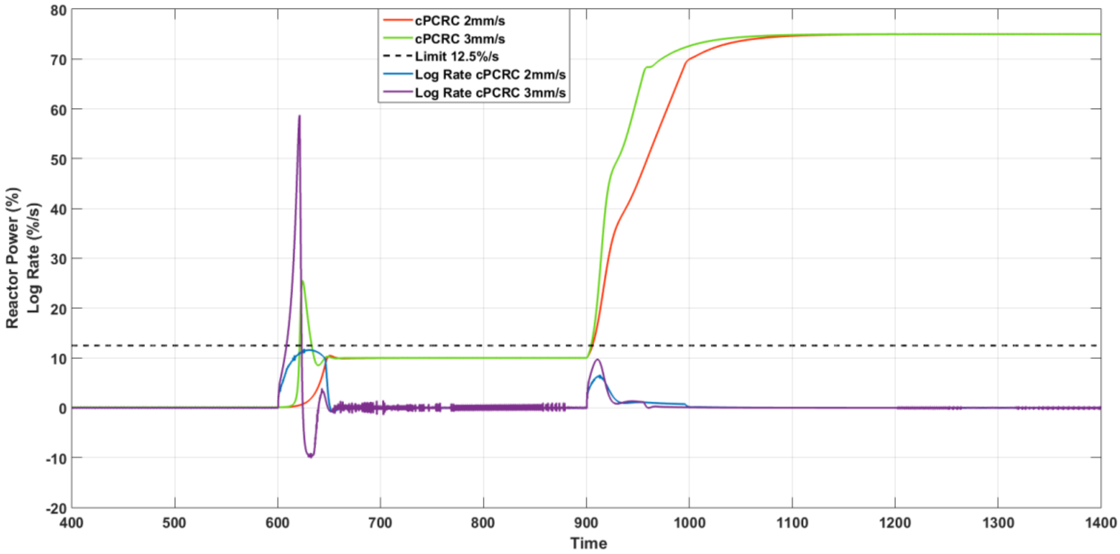

Figure 12. Comparison of different control rod speed values to limit the rate of power increment for conventional PCRC.

By referring to Figure 12, the rise time is too short and the rate of power change is more than 33.3%/s which caused the reactor to trip in real scenario at RTP [18]. The performance of Fuzzy PCRC (straight line) is optimized by using different values of control rod speeds as shown in Figure 13.

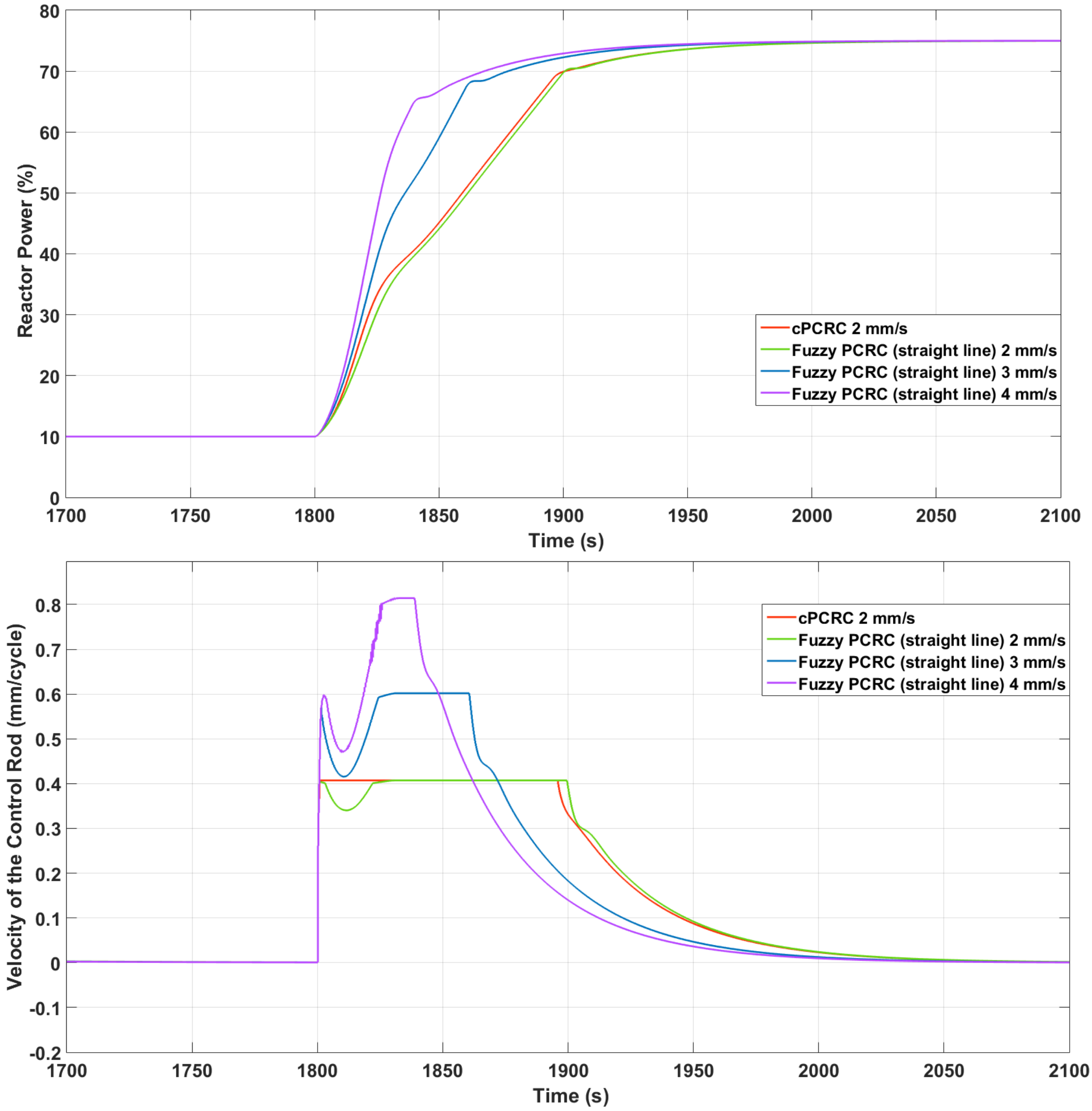

Figure 13. Different control rod speed values for nPCRC (by increasing the power to 75% FP).

In Figure 13, it can be observed that the tracking performance of Fuzzy PCRC (straight line) is improved by eliminating the unsmooth control surface and reducing the settling time when the control rod speed is increased from 2mm/s to 4mm/s. As a comparison in cPCRC, the rate of power change for the increased control rod speed from 3mm/s and 4mm/s is less than 12.5%/s. The performance of cPCRC and Fuzzy PCRC (straight line) with different control rod speed at 750kW is tabulated in Table 3.

Table 3. Performance summary for cPCRC and Fuzzy PCRC (straight line) at 750kW with different control rod speed.

Properties	*cPCRC with 2mm/s*	*Fuzzy PCRC (straight line) with 2mm/s*	*Fuzzy PCRC (straight line) with 3mm/s*	*Fuzzy PCRC (straight line) with 4mm/s*
Settling Time (T_s)	118.5 s	119.0 s	94.0 s	84.0 s
Percent Overshoot (%)	0.024 %	0.002 %	0.001 %	0.017 %
Rise Time (T_r)	84.5 s	86.0 s	58.5 s	50.0 s
Δe_{ce} (%)	0.383 %	0.365 %	0.191 %	0.166 %
Maximum Rate of Power Change (%/s) between 0.1 %FP - 10 %FP	11.580 %/s	11.000 %/s	11.520 %/s	11.800 %/s
Maximum Rate of Power Change (%/s) between 10 %FP - 75%FP	6.240 %/s	6.609 %/s	6.544 %/s	7.577 %/s

Overall, based on Table 3, a Fuzzy PCRC (straight line) with high control rod speed generally offers a better result than cPCRC. In addition, it can remove unwanted line noise for on CRDM when moving control rods and offer small settling time to reach demanded power.

6. Conclusion

In this work, a new design of PCRC is proposed by using fuzzy logic to improve the tracking performance of core power control at RTP. Instead of using a constant gain in cPCRC, Fuzzy PCRC offers generally better results which is able to reduce chattering noise maximum up to 56%. The core power control performance with Fuzzy PCRC can then be further improved by increasing the speed of the control rod. It has been proven in this work that the rate of power change at increased speed does not exceed 33.3 %/s which is the trip parameter.

7. References

[1] Jamil F, Abid M, Haq I, Khan A Q and Iqbal M 2016 Fault diagnosis of Pakistan Research Reactor-2 with data-driven techniques *Ann. Nucl. Energy* **90** p 433–440.

[2] Benítez-Read J S, Ruan D, Najera-Hernandez M, Perez-Clavel B, Pacheco-Sotelo J O and Lopez-Callejas R 2005 Comparison between a continuous and discrete method for the aggregation and defuzzification stages of a TRIGA reactor power fuzzy controller *Prog. Nucl. Energy* **46** p 309–320.

[3] Pérez-Cruz J H and Poznyak A 2008 Neural control for power ascent of a TRIGA reactor *Proc. Am. Control Conf.* p 2190–2195.

[4] Eom M, Chwa D and Baang D 2015 Robust disturbance observer-based feedback linearization control for a research reactor considering a power change rate constraint *IEEE Trans. Nucl. Sci.* **62** p 1301–1312.

[5] Coban R 2014 Power level control of the TRIGA Mark-II research reactor using the multifeedback layer neural network and the particle swarm optimization *Ann. Nucl. Energy* **69** p 260–266.

[6] Minhat M S, Mohd Subha N A, Hassan F and Mohamad Nordin N 2019 An improved control rod selection algorithm for core power control at Reaktor TRIGA PUSPATI *Symp. Control Syst. Signal Procesing* p 1-23.

[7] Minhat M S, Selamat H and Mohd Subha N A 2018 Adaptive control method for core power control in TRIGA Mark II reactor *IOP Conf. Ser. Mater. Sci. Eng.* **298** p 1-15.

[8] Luan X and Young A 2011 Load-following control of nuclear reactors based on Takagi-Sugeno fuzzy model *IFAC Proceedings Volumes* **44** p 8253-8258.

[9] Cavallaro F 2015 A Takagi-Sugeno fuzzy inference system for developing a sustainability index of biomass *Sustainability* **7** p 12359–12371.

[10] Eliasi H, Menhaj M B and Davilu H 2011 Robust nonlinear model predictive control for nuclear power plants in load following operations with bounded xenon oscillations *Nucl. Eng. Des.* v **241** p 533–543.
[11] Eliasi H, Menhaj M B and Davilu H 2012 Robust nonlinear model predictive control for a PWR nuclear power plant *Prog. Nucl. Energy* **54** p 177–185.
[12] Coban R 2010 Computational intelligence-based trajectory scheduling for control of nuclear research reactors *Prog. Nucl. Energy* **52** p 415–424
[13] Rojas-Ramírez E, Benítez-Read J S and Segovia-De-Los Ríos A 2013 A stable adaptive fuzzy control scheme for tracking an optimal power profile in a research nuclear reactor *Ann. Nucl. Energy* **58** p 238–245.
[14] Cammi A, Ponciroli R, Borio Di Tigliole A, Magrotti G, Prata M, Chiesa D and Previtali E 2013 A zero dimensional model for simulation of TRIGA Mark II dynamic response *Prog. Nucl. Energy* **68** p 43–54.
[15] Wang G, Wu J, Zeng B, Xu Z and Wu W 2016 State-space model predictive control method for core power control in pressurized water reactor nuclear power stations *Nucl. Eng. Technol.* **49** p134–140.
[16] Baang D, Suh Y and Park C 2017 Feedback power control for TRIGA-II research reactor *Trans. Korean Nucl. Soc. Spring Meet.* (Jeju, Korea) p 1-2.
[17] Baang D, Suh Y and Kim S H 2017 Power controller design and application to research reactor *Trans. Korean Nucl. Soc. Spring Meet.* (Gyeongju, Korea) p 1-2.
[18] Malaysia Nuclear Agency 2014 Safety analysis report for PUSPATI TRIGA reactor.
[19] Wai T C 2009 *Fuzzy Associative Memory Architecture* (Nanyang Technological University)
[20] Daher A, Hoblos G, Khalil M and Chetouani Y 2018 Parzen window distribution as new membership function for ANFIS algorithm- Application to a distillation column faults prediction *Chemom. Intell. Lab. Syst.* **51** p 241–248
[21] Nwankpa C E, Ijomah W, Gachagan A and Marshall S 2018 Activation functions : comparison of trends in practice and research for deep learning (*ArXiv 2018)* p 1–20
[22] Hatami E, Vosoughi N and Salarieh H 2016 Design of a fault tolerated intelligent control system for load following operation in a nuclear power plant *Electr. Power Energy Syst.* **78** p 864–872.
[23] Tan Y, Shuai C, Jiao L and Shen L 2017 An adaptive neuro-fuzzy inference system (ANFIS) approach for measuring country sustainability performance *Environ. Impact Assess. Rev.* **65** p 29–40.
[24] Jantzen J 1997 A robustness study of fuzzy control rules *Comp. Sci.* p 1–6.

Acknowledgments
This work was supported by a Fundamental Research Grant Scheme (FRGS) grant (FRGS/1/2017/TK04/UTM/02/55) from the Ministry of Higher Education, Malaysia. The author would like to thank all individuals who have contributed to this paper especially to Dr Nurul Adilla Binti Mohd Subha from Universiti Teknologi Malaysia and to the Malaysian Nuclear Agency under the Ministry of Energy, Science, Technology, Environment, and Climate Change, Malaysia (MESTECC) for the support.